

# Rapid $N_H$ changes in NGC 4151

S. Puccetti<sup>1,2</sup>, F. Fiore<sup>1</sup>, G. Risaliti<sup>3,4</sup>, M. Capalbi<sup>5</sup>,  
 M. Elvis<sup>4</sup>, F. Nicastro<sup>4,6</sup>

<sup>1</sup>*INAF-Osservatorio Astronomico di Roma, via Frascati 33, Monteporzio-Catone (RM), I00040 Italy.*

<sup>2</sup>*Dip. di Fisica, Università di Roma “Tor Vergata”, Via della Ricerca Scientifica, 00133 Rome, Italy.*

<sup>3</sup>*INAF-Osservatorio Astrofisico di Arcetri, Largo Enrico Fermi 5, Florence I-50125, Italy.*

<sup>4</sup>*Harvard-Smithsonian Center for Astrophysics, 60 Garden Street, Cambridge MA 02138.*

<sup>5</sup>*ASI Science Data Center, via Galileo Galilei, 00044 Frascati Italy.*

<sup>6</sup>*Instituto de Astronomía, Universidad Nacional Autonoma de Mexico,*

*Apartado Postal 70-264, Ciudad Universitaria, Mexico, D.F., CP 04510, Mexico.*

November 21, 2006

## ABSTRACT

We have analyzed the two longest (elapsed time  $\gtrsim 3$  days) BeppoSAX observations of the X-ray brightest Seyfert galaxy, NGC 4151, to search for spectral variability on time-scales from a few tens of ksec to years. We found in both cases highly significant spectral variability below  $\approx 6$  keV down to the shortest time-scales investigated. These variations can be naturally explained in terms of variations in the low energy cut-off due to obscuring matter along the line of sight. If the cut-off is modeled by two neutral absorption components, one fully covering the source and the second covering only a fraction of the source, the shortest time-scale of variability of a few days constrains the location of the obscuring matter to within  $3.4 \times 10^4$  Schwarzschild radii from the central X-ray source. This is consistent with the distance of the Broad Emission Line Region, as inferred from reverberation mapping, and difficult to reconcile with the parsec scale dusty molecular torus of Krolik & Begelman (1988). We have also explored a more complex absorption structure, namely the presence of an ionized absorber. Although the behaviour of the ionization parameter is nicely consistent with the expectations, the results are not completely satisfactory from the statistical point of view.

The overall absorption during the 2001 December observation is lower than in all other historical observations with similar 2-10 keV flux. This sug-

gests that absorption variability plays a crucial role in the observed flux variability of this source.

**Key words:** Galaxies: Seyfert – Galaxies: individual: NGC 4151 — X-rays: galaxies

## 1 INTRODUCTION

In the Unified Scheme for AGN (Antonucci 1993, Urry & Padovani 1995), type 2 narrow lines Active Galactic Nuclei (AGNs) are normal type 1 AGNs with both the characteristic broad emission lines and the optical to X-ray continuum observed through a column of gas and dust of density  $N_H \gtrsim 10^{22} \text{ cm}^{-2}$ . In this model, the absorption is located in a dusty torus at parsec distances from the central continuum (Krolik & Begelman 1988, Pier & Krolik 1992, Pier & Krolik 1993). Large variations of the obscuring screen are therefore not expected on time-scales much shorter than the crossing time at the dust sublimation radius ( $r_d = 4 \times L_{UV,46}^{1/2} T_{1500}^{-2.8} \times 10^{18} \text{ cm}$ , where  $L_{UV,46}$  is the ultraviolet luminosity in units of  $10^{46} \text{ erg s}^{-1}$  and  $T_{1500}$  is the grain evaporation temperature in units of 1500 K, Barvainis 1987). However, Risaliti, Elvis & Nicastro (2002) found that 23/24 X-ray absorbed (Compton “thin”, i.e.  $N_H \lesssim 10^{24} \text{ cm}^{-2}$ ) AGNs showed  $N_H$  variability by a factor 2-3, and, most interestingly, that several objects varied on time-scales of months (but see the case of NGC 4388 for even shorter variability time-scales: Elvis et al. 2004), implying a limit to the distance  $r$  of the absorber from the X-ray source of  $4.5 \times 10^{16} \frac{M_\bullet}{10^9 M_\odot} \left( \frac{n_e}{10^6 \text{ cm}^{-3}} \right)^2 \left( \frac{N_H}{5 \times 10^{22} \text{ cm}^{-2}} \right)^{-2} \text{ cm}$ . Therefore Risaliti, Elvis & Nicastro (2002) suggested that the absorber might be located in cool clouds present in an accretion disk wind on the scale of the Broad Emission Line Region (BELR). This echoes the model of Kartje, Königl & Elitzur (1999), which predicts  $N_H$  variability down to a time-scales of days. Variations of the overall level of the absorption may also be expected in the case of an ionized absorber responding to variations of the continuum level (see e.g. Nicastro et al. 1999, Schurch & Warwick 2002). An accurate analysis of the temporal behaviour of the X-ray absorber can help us to gain precious information on its physics, size, geometry and location. Unfortunately, this has been possible so far in a handful of cases only (e.g. NGC 4388, Elvis et al. 2004, NGC 1365, Risaliti et al. 2005, Mkn 348, Smith et al. 2001), because of the strong parameter degeneracy in complex, multi-component spectral fittings, in particular between the absorber and the continuum parameters. High statistics, broad-band observations are crucial to remove this degeneracy. To this purpose, we have

analyzed two BeppoSAX long (elapsed time  $\gtrsim 3$  days) observations of the bright Seyfert galaxy, NGC 4151, which are particularly well suited to further investigate this issue. In this paper we focus on the search for variability of the absorber on time-scales from a few tens of ksec to years.

NGC 4151 is one of the brightest Seyfert galaxy in the sky in the X-ray band, and for this reason it has been studied in detail by all X-ray missions since the discovery of its X-ray emission in the 1971 (Gursky et al. 1971). The intrinsic continuum has historically been parameterized by an absorbed power law, with variable intensity and photon index ( $1.3 < \Gamma < 1.9$ , Ives, Sandford & Penston 1976, Barr et al. 1977, Paciesas, Mushotzky & Pelling 1977, Perola et al. 1986, Yaqoob, Warwick, & Pounds 1989, Fiore et al. 1990, Schurch and Warwick 2002, Zdziarski et al. 2002). A strong narrow iron  $K_{\alpha}$  line is present in the spectrum. This line has an intensity of  $1.8 \times 10^{-4}$  ph cm $^{-2}$  s $^{-1}$  (HETGS (i.e. High-Energy Transmission Grating Spectrometer, Canizares 2000) Ogle et al. 2000). The narrow core of the line is unresolved, with FWHM= $<2000$  km s $^{-1}$ . The Fe  $K_{\alpha}$  intensity remains constant over short-medium (days-months) time-scales and varies by  $\sim 25\%$  on time-scales of about one year (Perola et al. 1986, Zdziarski et al. 2002, Schurch and Warwick 2002, Takahashi, Inoue and Dotani 2002, Schurch et al. 2003). These time-scales suggest that the Fe  $K_{\alpha}$  line arises in a region at a distance  $r \sim 10^{17}$  cm from the nucleus. A Compton reflection component has been detected in the spectrum of NGC 4151 by Zdziarski et al. (2002), Schurch and Warwick (2002). At energies above 50 keV the continuum becomes steeper, and this change in slope can be modelled by an exponential cut-off with e-folding energy of 70–250 keV (Zdziarski et al. 1996).

The nuclear power-law spectrum is heavily absorbed at  $E \leq 6$  keV by a photoelectric absorption due to a large amount of material along the line of sight ( $N_H \sim 10^{22} - 10^{23}$  cm $^{-2}$ ). A single absorber does not provide a good fit, as recognized since the first Einstein observations (SSS, Holt et al. 1980). A better description of the spectrum is provided by an inhomogeneous absorber, which allows some fraction of the nuclear X-ray continuum to emerge with significantly less attenuation than the rest of the continuum. Both a partial covering absorber (Holt et al. 1980, Perola et al. 1986, Zdziarski et al. 2002) and an ionized absorber (Yaqoob, Warwick, & Pounds 1989, Weaver et al. 1994, Schurch and Warwick 2002) have been proposed in the past. Part of the emission is due to extended kpc-scale emission associated with the narrow line region (Elvis, Briel & Henry, 1983, Ogle et al. 2000). Interestingly, changes of the absorbing screen(s) on time-scales of days to years have been often reported in the past (Barr et al. 1977, Fiore et al. 1990, Yaqoob et al. 1993, Schurch & Warwick 2002).

These changes have been interpreted in terms of creation and destruction of cold filaments and clouds in the BELR (Barr et al. 1977), or in terms of their orbital motion (Holt et al. 1980, Lawrence & Elvis 1982). In the latter case, the inhomogeneous absorber consists of a large number of discrete clouds, each much smaller than the size of the X-ray source. The number of the clouds that, at any time, cover a given line of sight is distributed according to the Poisson statistics. Column density variations, in this scenario, are simply due to statistical fluctuations of the number of clouds along the line of sight. The thickness and size of the absorbing clouds can therefore be estimated by measuring amplitude and time-scales of the column density variations. In models of a partially ionized absorber the variations in the underlying ionizing continuum change the optical depth of the absorber along the light of sight and so simulate a change in equivalent H column density, when the spectra are modelled with a neutral absorber. In this scenario, Schurch & Warwick (2002) interpret the spectral variability observed in a ASCA long look in terms of changes of the ionization state in response of variations of the underlying continuum flux. This interpretation relies on the assumption of a constant underlying continuum shape, evaluated using a previous BeppoSAX broader band observation. In this paper we report on changes in the obscuring column density on time-scales of a few days, which strongly constrain the geometry of the absorber. Thanks to the high statistics and broad spectral coverage we were able for the first time to investigate the nature of the observed variability without resorting on any a-priori assumption on the continuum emission.

The structure of this paper is the following: Section 2 gives some details on the data reduction, Section 3 illustrates the method used for the data analysis and presents the results of the temporal and spectral analysis, Section 4 is devoted to the discussion of our results and conclusions.

## 2 OBSERVATIONS AND DATA REDUCTION

To look for changes in the absorber(s) of NGC 4151 and to further investigate on its origin and geometry, we have selected the two longest observations performed with the BeppoSAX Narrow Field Instruments (Table 1), LECS (0.1-10 keV, Parmar et al. 1997), MECS (1.3-10 keV, Boella et al. 1997) and PDS (13-200 keV, Frontera et al. 1997), which have good sensitivity from 0.1 to at least 100 keV. Because of the complexity of the spectrum, an energy coverage as broad as possible is the key to obtain a good constrain on the absorption

**Table 1.** Observation log.

Instrument	channels	Energy range	Net counts $s^{-1}$	Exposure (s)
1996 July 6-9				
LECS	41-370	0.45-4 keV	$0.109 \pm 0.003$	8960
MECS	37-227	1.65-10.5 keV	$1.446 \pm 0.004$	73620
PDS	50-580	15-200 keV	$4.09 \pm 0.03$	35160
2001 December 18-20				
LECS	41-370	0.45-4 keV	$0.395 \pm 0.003$	43300
MECS	37-227	1.65-10.5 keV	$2.070 \pm 0.004$	114860
PDS	50-580	15-200 keV	$5.10 \pm 0.02$	53290

models. The first observation was performed between 1996 July 6 and 9 for a total elapsed time of  $\sim 300$  ksec. During the observation the 2-4 keV flux increased by a factor  $\sim 3$ , and therefore this observation is particularly well suited to search for spectral variability. The second observation was a target of opportunity observation (ToO) performed between 2001 December 18 and 20, for a total elapsed time of  $\sim 275$  ksec, during a NGC 4151 outburst in the soft X-rays. This outburst was serendipitously detected by the BeppoSAX Wide Field Cameras, and a ToO observation of the source with the Narrow Field Instruments was promptly performed. In this observation the signal to noise is particularly good and allows us to search for small spectral variation, and for variation on short time-scales.

The 1996 July observation was performed with MECS units 1, 2 and 3, while the 2001 December observation was performed with MECS units 2 and 3 only (on 1997 May 6 a technical failure caused MECS unit 1 to be switched off); data from the units were combined after gain equalization. The LECS was operated during dark time only, therefore LECS exposure times are smaller than MECS ones. Table 1 gives the LECS, MECS and PDS exposure times and the mean count rates.

Standard data reduction was performed using the SAXDAS software package version 2.0 following Fiore, Guainazzi & Grandi (1999). In particular, data are linearized and cleaned of Earth occultation periods (we accumulated data for Earth elevation angles  $> 5$  degrees) and unwanted periods of high particle background (satellite passages through the South Atlantic Anomaly and periods with magnetic cut-off rigidity  $> 6$  GeV/c).

NGC 4151 lies 5 arcmin south of the relatively bright BL Lac object 1E1207.9+3945 (0.3-3.5 keV flux of  $1.5 \times 10^{-12}$  erg cm $^{-2}$  s $^{-1}$ , Gioia et al. 1990) and  $\sim 5.2$  arcmin south of the galaxy NGC 4156 (which is  $\sim 20$  times fainter than NGC 4151, Elvis et al. 1981, Fabbiano et al. 1992). To study the possible contamination from these two sources we compared the LECS and MECS spectra extracted from regions of 2, 3 and 4 arcmin radii. The

spectra are all consistent with each other in shape and therefore we conclude that the contamination of the nearby sources is negligible, even in the 4 arcmin radius spectra. Since these spectra provide the best signal to noise, we use them in the following analysis.

Background spectra were extracted in detector coordinates from high Galactic latitude ‘blank’ fields (98-11 release) using regions equal in size to the source extraction region. We have compared the mean level of the background in the LECS and MECS “blank fields” observations to the mean level of the background in the NGC 4151 observations using source free regions at various positions in the detectors. The “local” MECS, LECS background count rates are within a few per cent of those in the “blank fields”.

The PDS data were reduced using the “variable risetime threshold” technique to reject particle background (see Fiore, Guainazzi & Grandi 1999). To check the reliability of the background subtraction in the PDS spectra we looked at the spectrum between 200 and 300 keV, where the effective area of the PDS to X-ray photons is small and therefore the source contribution is negligible. After background subtraction we obtain a count rate of  $0.01 \pm 0.01$  counts  $s^{-1}$ , for the 1996 July observation and  $0.003 \pm 0.009$  counts  $s^{-1}$  for the 2001 December observation, fully consistent with the expected value of 0. The BL Lac object 1E1207.9+3945 and the galaxy NGC 4156 contribute less than a few per cent to the PDS flux, based on the extrapolation of the 2-10 keV spectrum of these sources to higher energies, assuming a power law spectrum with  $\Gamma = 2.1$  (Perlman et al. 1996) and a 7 keV exponential spectrum (Burstein et al. 1997) respectively. NGC 4151 is detected with a signal to noise ratio  $S/N \gtrsim 3$  up to 130–140 keV in the two observations.

Spectral fits were performed using the XSPEC 11.2.0 software package and the most recent responses (1999 December release). For both LECS and MECS we used the standard on-axis responses, since the source is close to the default pointing position (within 5 raw pixels, i.e. 40 arcsec). LECS and MECS spectra were binned following two criteria: (a) allowing at least four channels per resolution element at all energies, when possible, and (b) to obtain at least 20 counts per energy channels.

Constant normalization factors have been introduced in the fitting models in order to take into account the intercalibration systematics between the instruments (Fiore, Guainazzi & Grandi 1999). The normalization factor between the LECS and the MECS instruments, assuming the MECS as a reference, has been obtained by fitting the LECS and MECS spectra in the common 1.65–4 keV band with a simple power law model. We obtained a normalization factor of  $0.40 \pm 0.02$  for the 1996 July observation and a factor of  $0.60 \pm 0.01$  for the 2001 December

observation. Accordingly, in all the following fits the LECS-MECS factor is constrained to vary in the above ranges for the 1996 July observation and for the 2001 December observation respectively. The LECS-MECS normalization factor is somewhat lower than usually assumed (see Fiore, Guainazzi & Grandi 1999), due to the adopted LECS source extraction region of radius 4 arcmin, smaller than the typical one (because of confusion problems, see above). The normalization factor adopted between the PDS and the MECS instruments is constrained to vary between 0.72 and 0.87, as recommended (see Fiore, Guainazzi & Grandi 1999).

In the spectral fits we used the LECS between 0.45-4 keV (channels 41-370), MECS between 1.65-10.5 keV (channels 37-227), and the PDS between 15-200 keV (channels 50-580). Errors throughout the paper are quoted at a significance level of 90% for two interesting parameters ( $\Delta\chi^2 = 4.61$  Lampton et al. 1976), unless differently specified.

### 3 DATA ANALYSIS

The aim of this paper is to search for variations of the absorber(s) on time-scales from a few tens of ksec to years. The total absorbing column density measured toward NGC 4151 ranges from a few  $10^{22}$  cm $^{-2}$  to a few  $10^{23}$  cm $^{-2}$  and the corresponding photoelectric cut-off lies in the 2-4 keV energy range. This band is therefore best suited to monitor changes in the absorber. The 6-10 keV and 15-100 keV bands, being less affected by photoelectric absorption can be used to monitor the continuum, normalization and power law photon index.

#### 3.1 Light curves analysis

Light curves of the count rate in the three energy bands 2-4 keV, 6-10 keV, 15-100 keV, and the softness ratios 2-4 keV/6-10 keV and 6-10 keV/15-100 keV, are plotted in figures 1 and 2 in bins of 5500 seconds ( $\sim 1$  satellite orbit). The analysis of both count rate and softness ratio light curves indicates large spectral variations on time-scales from a few tens of ksec to a few days.

On longer time-scales (i.e. the 4.5 years between the two observations), we find similar results. The 6-10 keV count rates in the intervals A and B of the 1996 July observation are similar to the corresponding count rates recorded during the 2001 December observation (see figures 3), as well as the 6-10 keV/15-100 keV softness ratios. Conversely, the 2-4 keV/6-

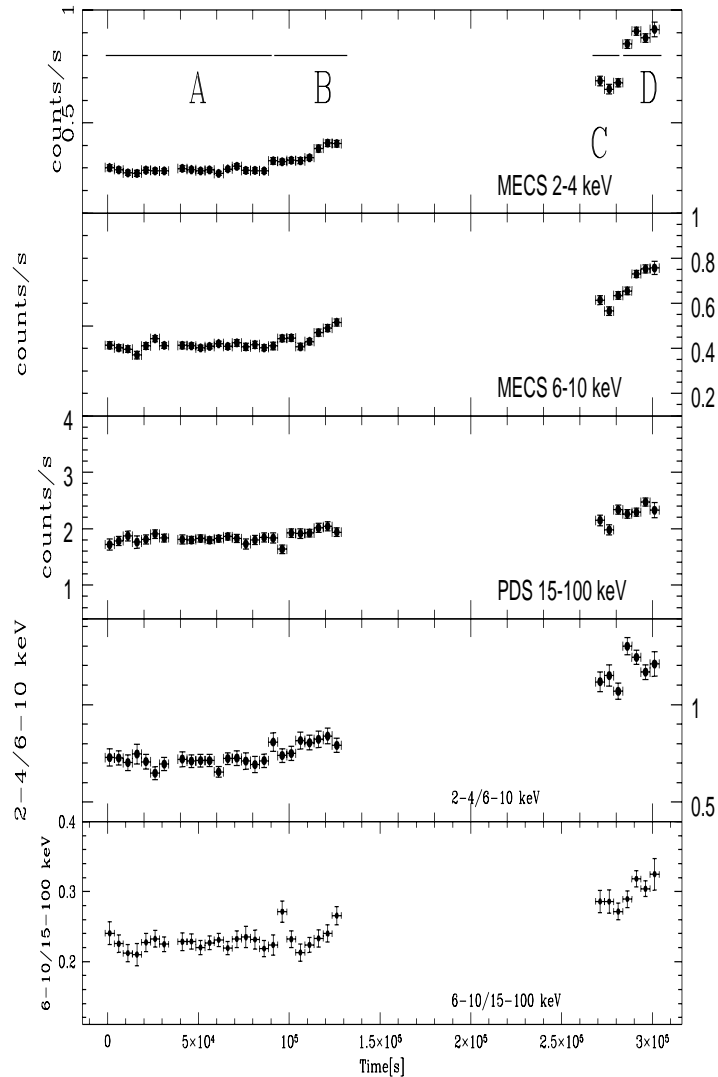


**Figure 1.** Light curves of the 1996 July observation in bins of 5500 seconds ( $\sim 1$  satellite orbit). From top to bottom: MECS 2-4 keV count rate, MECS 6-10 keV count rate, PDS 15-100 keV half detector count rate, 2-4 keV/6-10 keV softness ratio, 6-10 keV/15-100 keV softness ratio. Capital letters and lines in the top panel indicate the time intervals selected for a time-resolved spectral analysis.

10 keV softness ratios are different by a factor  $\sim 2$  (see figure 4). The similarity of the higher energy count rates (and 6-10 keV/ 15-100 keV softness ratios) suggests a comparable photon index in the range  $\sim 1.75$ -1.85 (assuming a simple power law model reduced at low energy by a uniform column of cold gas). On the other hand, the difference in the 2-4 keV/6-10 keV ratios can be naturally explained by secular changes of the absorber of  $\gtrsim 60\%$ .

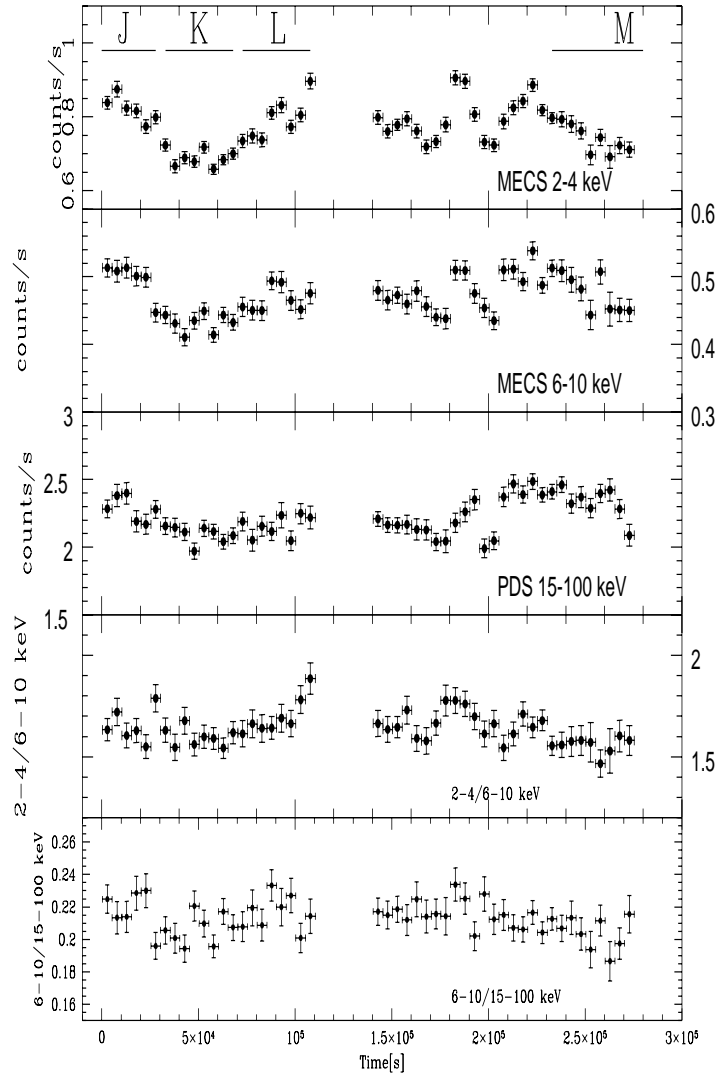


**Figure 2.** Light curves of 2001 December observation in bins of 5500 seconds ( $\sim 1$  satellite orbit). From top to bottom: MECS 2-4 keV count rate, MECS 6-10 keV count rate, PDS 15-100 keV half detector count rate, 2-4 keV/6-10 keV softness ratio, 6-10 keV/15-100 keV softness ratio. Capital letters and lines in the top panel indicate the time intervals selected for a time-resolved spectral analysis.

### 3.2 Spectral analysis

The statistics of the spectra extracted in 5500 s bins is not high enough to constrain complex models. To characterize the spectral variability we therefore accumulated spectra in contiguous time intervals when the source does not display large spectral variations. We selected four time intervals for each of the two observations to perform a time resolved spectral analysis (indicated as A, B, C and D in figure 1 and as J, K, L, M in figure 2). The counts spectra in these time intervals are plotted in the upper panels of figures 5 and 6.

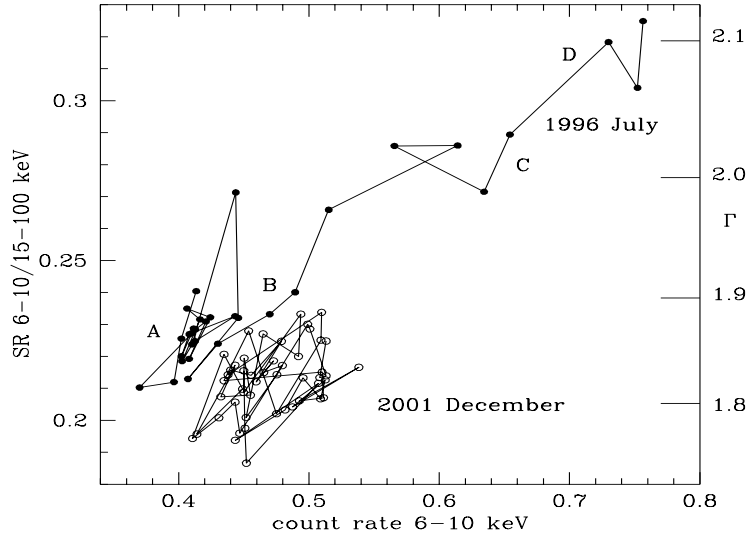


**Figure 3.** 6-10 keV/15-100 keV softness ratio versus the count rate in 6-10 keV range. The open dots indicate the 2001 December observation, the solid dots indicate the 1996 July observation. The lines on the right hand side are the 6-10 keV/15-100 keV softness ratio expected from a power law model with photon index  $\Gamma$ , reduced at low energy by photoelectric absorption from neutral gas of column density  $N_H = 10^{23} \text{ cm}^{-2}$ .

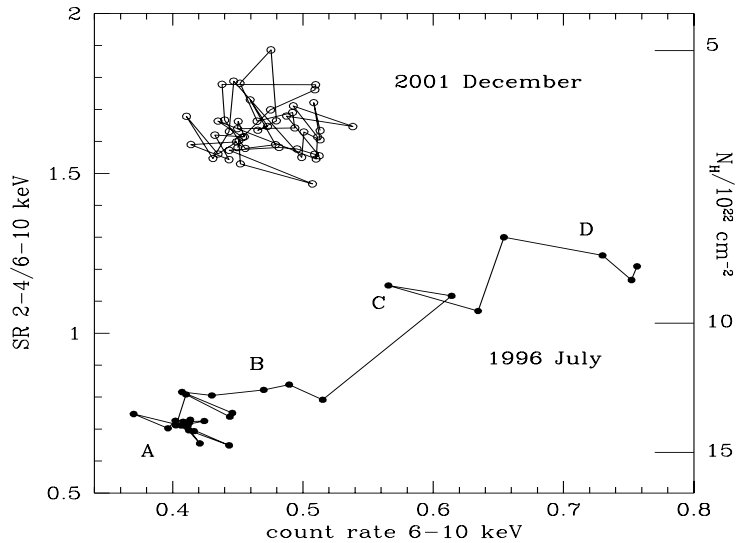


**Figure 4.** 2-4 keV/6-10 keV softness ratio versus the count rate in 6-10 keV range. The open dots indicate the 2001 December observation, the solid dots indicate the 1996 July observation. The lines on the right hand side are the 2-4 keV/6-10 keV softness ratio expected from a power law model with photon index 1.8, reduced at low energy by photoelectric absorption from neutral gas of column density  $N_H$ .

The lower panels plot the same spectra normalized to the lower count rate spectrum of each observation. The largest variations are seen below  $\approx 6$  keV, thus suggesting variations of the absorber(s).

The comparison of figures 5 and 6 suggests that the absorber variations during the 2001 December observation are smaller than those in the 1996 July observation, but qualita-

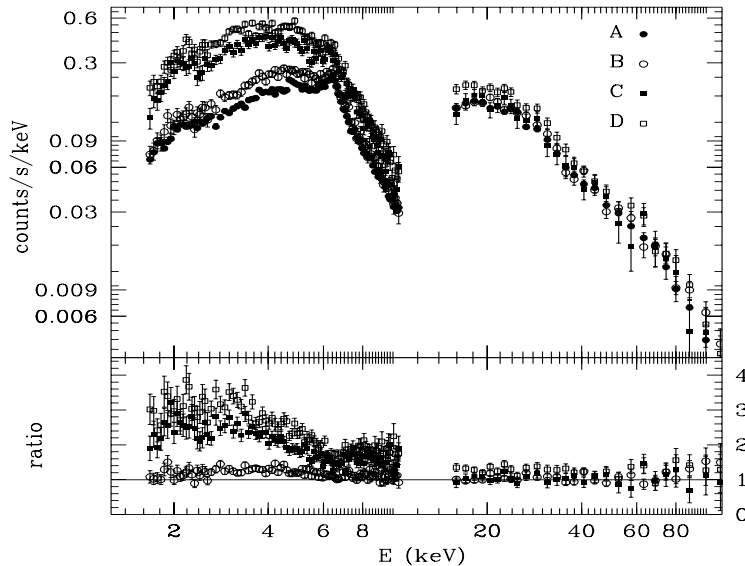


**Figure 5.** 1996 July observation. Top panel: counts spectra of the data in the selected time intervals indicated in figure 1. Bottom panel: ratio between the counts spectra to the lower counts spectrum, A. LECS data are not shown for the sake of clarity (statistical scatter is comparable with the observed variability).

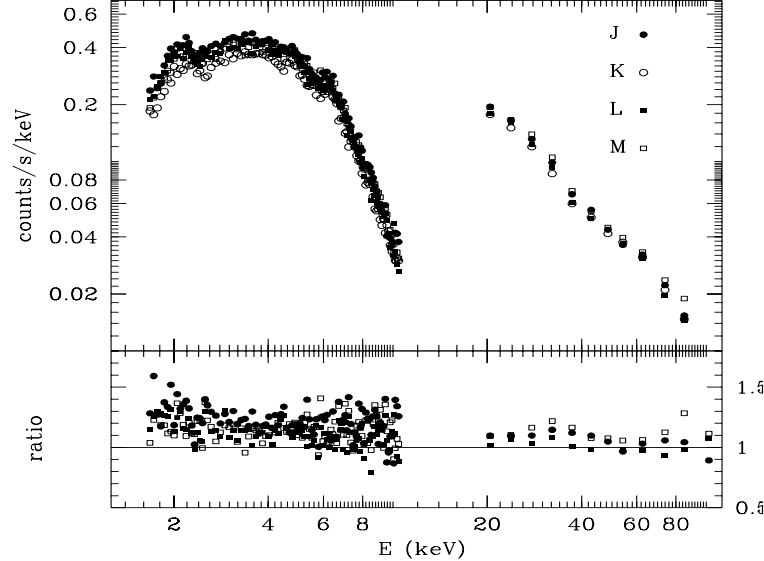


**Figure 6.** 2001 December observation. Top panel: counts spectra of the data in the selected time intervals indicated in figure 2. Bottom panel: ratio between the counts spectra to the lower counts spectrum, K. LECS data are not shown for the sake of clarity (statistical scatter is comparable with the observed variability).

tively similar. To fully characterize the observed spectral variations we performed a detailed spectral analysis of the spectra plotted in figures 5 and 6. We have adopted a model including the following components. The hard X-ray continuum is described by a power-law with an exponential high-energy cut-off plus a neutral Compton reflection component (the PEXRAV model in XSPEC, Magdziarz & Zdziarski 1995). The latter component can be safely assumed constant on time-scales from days to months (see e.g. Johnson et al. 1997)

and therefore its normalization has been fixed to the best fit value found fitting the spectra of each complete observation. A narrow iron  $K_{\alpha}$  emission line with energy set to 6.4 keV (rest frame) is added to this continuum.

The soft X-ray continuum is described by two components, a thermal bremsstrahlung component (Elvis et al. 1990, Weaver et al. 1994 and references therein), and a scattering component (Weaver et al. 1994). The thermal component can be safely assumed constant on the time-scales spanned by our observations and therefore we fixed temperature and normalization to the best fit values found by fitting the total 2001 December spectrum ( $T=0.18$  keV and a 0.4-4 keV flux of  $1.8 \times 10^{-12}$  erg cm $^{-2}$  s $^{-1}$ ). The low energy scattering component, parameterized by a power law, is likely produced by scattering of the nuclear power law by warm-hot gas distributed on scales greater than parsec (Ogle et al. 2000, Yang et al. 2001). Therefore, also this component can be safely assumed constant on the time-scales spanned by our observations. We fixed its photon index to 1.7 and the normalization to the best fit values found by fitting the total spectra (0.4-4 keV flux of  $6.1 \times 10^{-12}$  erg cm $^{-2}$  s $^{-1}$  and of  $4.5 \times 10^{-12}$  erg cm $^{-2}$  s $^{-1}$  for the 1996 July and the 2001 December observations, respectively).

The complex absorber has been parameterized in three different ways: A) two neutral components, one covering the nucleus totally and the other covering the nucleus only partly; B) one neutral absorber and one ionized absorber both covering the nucleus totally; and C) one ionized absorber covering the nucleus totally and one neutral absorber covering the nucleus only partly. A Galactic column density along the line of sight of  $N_H(gal) = 2.1 \times 10^{20}$  cm $^{-2}$  (Murphy et al. 1996) has been added to the model in all cases.

Models A) and B) have seven free parameters: the photon index  $\Gamma$ , normalization and the energy of the cut-off of the nuclear continuum, three parameters for the absorber ( $N_H$ ,  $N_{Hc}$ ,  $c_v$ , or  $N_{H1}$ ,  $N_{Hw}$ , and the ionization parameter  $\xi$ ) and the normalization of the iron  $K_{\alpha}$  line. Model C) has one more free parameter (the covering fraction of the neutral absorber).

Model A) provided the smallest  $\chi^2$  in both 1996 July and 2001 December observations. We then discuss first the results of this series of fits and then compare them with the results obtained using models B) and C). Tables 2 and 3 give the best fit values of  $N_H$ ,  $N_{Hc}$ ,  $c_v$ ,  $\Gamma$ , along with the  $\chi^2$ , the count rate and the flux in the 6-10 keV band, for the four spectra selected in each observation. In all cases the fits are acceptable at a confidence level better than 3%. Figure 7 shows the 68%, 90%, and 99%  $\chi^2$  confidence contours of  $N_{Hc}$  versus  $\Gamma$ ,  $N_H$  versus  $N_{Hc}$  and  $C_v$  versus  $N_H$  for the 1996 July and the 2001 December observations.

**Table 2.** 1996 July observation: the best fit parameters of model A.

spectrum	$\chi^2$	$N_H^a$	$N_H c^b$	$c_v^c$	$\Gamma^d$	$c_{6-10}^e$	$F_{6-10}^f$
A	149.20/151	$6.2 \pm 1.0$	$30.3 \pm 9.0$	$0.71 \pm 0.04$	$1.79 \pm 0.03$	0.41	5.48
B	147.74/138	$4.6 \pm 1.7$	$14.0 \pm 8.0$	$0.7 \pm 0.2$	$1.77 \pm 0.04$	0.45	6.03
C	119.10/118	$2.6 \pm 1.0$	$11.6 \pm 8.1$	$0.6 \pm 0.2$	$1.82 \pm 0.04$	0.64	8.22
D	124.29/118	$2.4 \pm 0.9$	$10.0 \pm 7.3$	$0.6 \pm 0.2$	$1.77 \pm 0.03$	0.73	9.75

<sup>a</sup> column density of the totally covering absorber in unit of  $10^{22} \text{ cm}^{-2}$ , <sup>b</sup> column density of the partial covering absorber in unit of  $10^{22} \text{ cm}^{-2}$ , <sup>c</sup> covering factor, <sup>d</sup> photon index, <sup>e</sup> 6-10 keV count rate, <sup>f</sup> MECS 6-10 keV flux in  $10^{-11} \text{ erg cm}^{-2} \text{ s}^{-1}$ .

**Table 3.** 2001 December observation: the best fit parameters of model A.

spectrum	$\chi^2$	$N_H^a$	$N_H c^b$	$c_v^c$	$\Gamma^d$	$c_{6-10}^e$	$F_{6-10}^f$
J	134.22/136	$1.4 \pm 0.3$	$6.1 \pm 2.3$	$0.5 \pm 0.1$	$1.80 \pm 0.04$	0.50	10.01
K	134.43/136	$1.6 \pm 0.4$	$6.3 \pm 2.4$	$0.6 \pm 0.1$	$1.82 \pm 0.04$	0.43	8.48
L	168.93/136	$1.6 \pm 0.3$	$6.7 \pm 2.3$	$0.50 \pm 0.09$	$1.82 \pm 0.03$	0.465	9.19
M	152.55/135	$2.2 \pm 0.3$	$10.8 \pm 5.6$	$0.41 \pm 0.08$	$1.81 \pm 0.03$	0.49	9.71

<sup>a</sup> column density of the totally covering absorber in unit of  $10^{22} \text{ cm}^{-2}$ , <sup>b</sup> column density of the partial covering absorber in unit of  $10^{22} \text{ cm}^{-2}$ , <sup>c</sup> covering factor, <sup>d</sup> photon index, <sup>e</sup> 6-10 keV count rate, <sup>f</sup> MECS 6-10 keV flux in  $10^{-11} \text{ erg cm}^{-2} \text{ s}^{-1}$ .

During both observations the photon index is constant at a confidence level better than 68% while both absorbers undergo significant changes. During the 1996 July observation  $N_{Hc}$  and  $N_H$  both change by  $\sim 60\%$  at a confidence level better than 99% from A to C. Significant (at a confidence level better than 90 %) but smaller changes are also present from spectra A to B. On the other hand, the covering factor  $c_v$  is consistent with a constant value within the relatively large errors, especially for spectra C and D. During the 2001 December observation we detect significant changes of the absorbers, despite smaller flux variations.  $N_{Hc}$  and  $N_H$  change at a confidence level better than 90% by  $\sim 60\%$  and  $\sim 35\%$  from L to M respectively. The covering factor changes by 25% at a confidence level better than 90% from J to M.

We remark that statistically significant changes of the absorber parameters have been obtained leaving the power law continuum parameters free to vary and therefore we can exclude that they are spurious results of subtle variations of the continuum shape. Having assessed this, we can fix the continuum shape to obtain a better constraint of the absorbers parameters. Since the covering factor turned out to be constant or limited within a narrow range, we also fix it in the next series of fits. These new constraints do not worsen the fit, the total  $\chi^2$  increasing by 14 for 16 additional degrees of freedom. Figure 8 shows the  $N_H - N_{Hc}$   $\chi^2$  confidence contours for the two observations for this series of fits. The magnitude of the variations of both parameters is similar to those reported above, but of course now

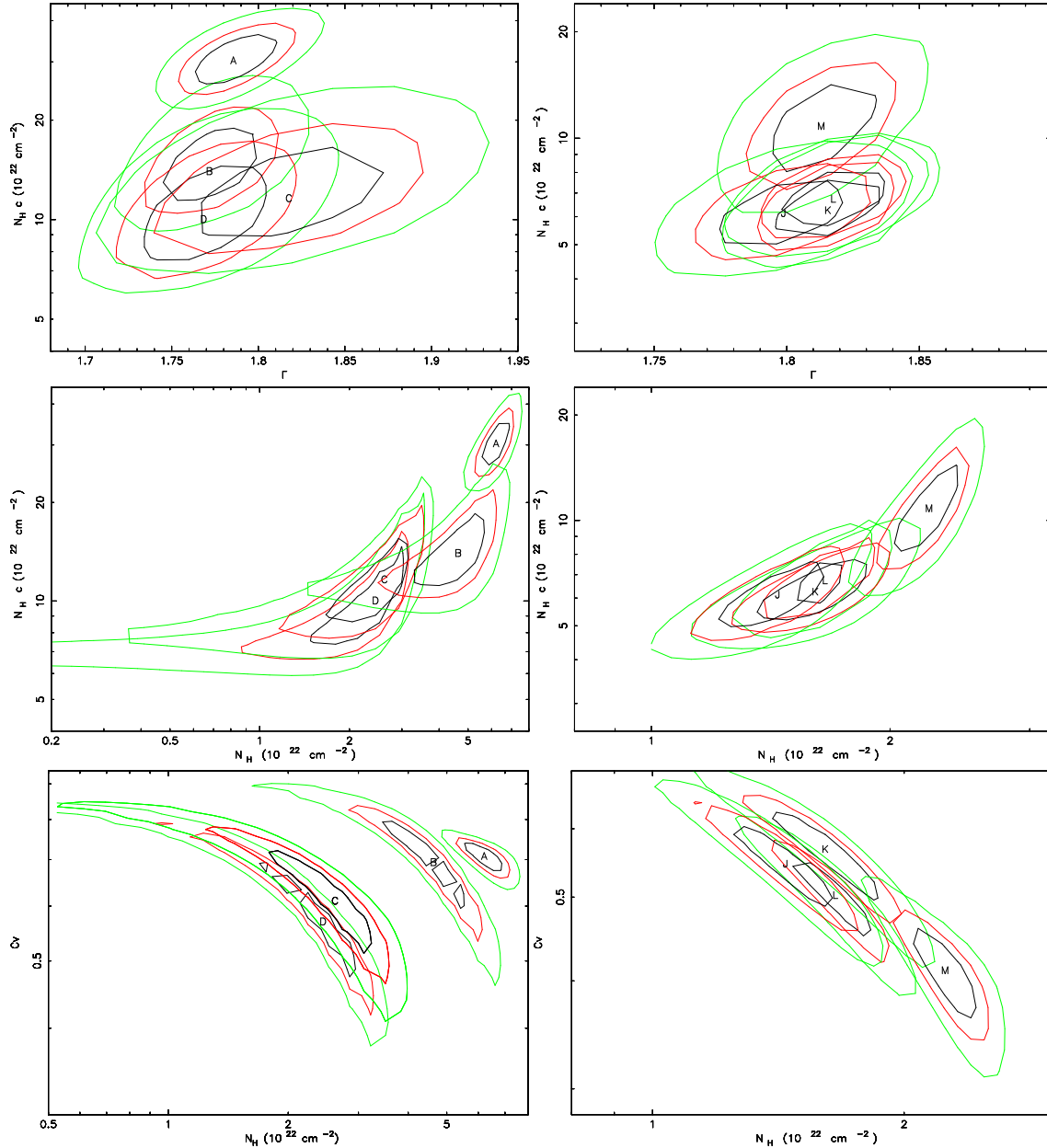


**Figure 7.** 68%, 90% and 99%  $\chi^2$  confidence contours of the partial covering absorber versus the photon index (upper panels), partial covering absorber versus the totally covering absorber (central panels) and partial covering factor versus the totally covering absorber (lower panels) for the 1996 July observation (left panels) and the 2001 December observation.

the  $\chi^2$  contours are smaller, and therefore the variations are more statistically significant. In the July 1996 observation the variations of  $N_H$  and  $N_{Hc}$  seems correlated one to the other (Figure 8). This may appear unexpected, but it should be considered that real absorbers would have smooth edges and therefore  $N_H$  would vary smoothly, covering the source with a continuous set of  $N_H$  values. If this is the case, it is not truly surprising to find a correlation between the two parameters of our simple representation of this complex structure.

In addition to the partial covering model (A), we now explore two versions of a more

**Table 4.** 1996 July observation: the best fit parameters of model B.

s <sup>a</sup>	$\chi^2$	$N_{H1}^b$	$N_H w^c$	$\xi^d$	$\Gamma^e$	$\chi^2 f$	$N_{H1}^g$	$N_H w^h$	$\xi^i$
A	229.5/151	$6.0 \pm 3.7$	$20.0 \pm 7.9$	$210 \pm 470$	$1.69 \pm 0.02$	235.1/152	$6.3 \pm 3.7$	$20.6 \pm 7.9$	$220 \pm 430$
B	146.6/138	$<5.2$	$17.6 \pm 4.0$	$45 \pm 170$	$1.72 \pm 0.03$	146.8/139	$<5.3$	$17.3 \pm 4.0$	$40 \pm 100$
C	123.4/118	$<2.2$	$15.4 \pm 5.7$	$140 \pm 270$	$1.74 \pm 0.06$	124.2/119	$<1.8$	$14.9 \pm 4.6$	$140 \pm 260$
D	139.3/118	$<3.3$	$13.1 \pm 3.2$	$530 \pm 680$	$1.70 \pm 0.03$	139.5/119	$<4.0$	$13.5 \pm 4.9$	$520 \pm 630$

<sup>a</sup> time interval, <sup>b</sup> column density of the fully covering absorber in unit of  $10^{22} \text{ cm}^{-2}$ , <sup>c</sup> column density of uniform ionized absorber in unit of  $10^{22} \text{ cm}^{-2}$ , <sup>d</sup> absorber ionization parameter ( $L/nR^2$ , see Done et al. 1992), <sup>e</sup> photon index, <sup>f</sup>  $\chi^2$  for  $\Gamma$  fixed to 1.71, <sup>g</sup>, <sup>h</sup> and <sup>i</sup> as <sup>b</sup>, <sup>c</sup> and <sup>d</sup> respectively, for  $\Gamma$  fixed to 1.71.

**Table 5.** 2001 December observation: the best fit parameters of model B.

s <sup>a</sup>	$\chi^2$	$N_{H1}^b$	$N_H w^c$	$\xi^d$	$\Gamma^e$	$\chi^2 f$	$N_{H1}^g$	$N_H w^h$	$\xi^i$
J	144.7/136	$1.5 \pm 0.3$	$7.8 \pm 2.6$	$360 \pm 310$	$1.73 \pm 0.03$	146.6/137	$1.5 \pm 0.3$	$8.3 \pm 2.6$	$370 \pm 330$
K	141.9/136	$1.7 \pm 0.3$	$9.8 \pm 2.5$	$460 \pm 320$	$1.77 \pm 0.02$	144.0/137	$1.8 \pm 0.3$	$9.1 \pm 2.5$	$440 \pm 320$
L	187.9/136	$1.8 \pm 0.3$	$9.3 \pm 3.1$	$610 \pm 270$	$1.77 \pm 0.03$	190.4/137	$1.8 \pm 0.3$	$8.6 \pm 2.9$	$590 \pm 510$
M	169.6/135	$2.0 \pm 0.4$	$8.7 \pm 4.7$	$560 \pm 780$	$1.74 \pm 0.02$	171.2/136	$2.1 \pm 0.4$	$9.4 \pm 3.5$	$640 \pm 680$

<sup>a</sup> time interval, <sup>b</sup> column density of the fully covering absorber in unit of  $10^{22} \text{ cm}^{-2}$ , <sup>c</sup> column density of uniform ionized absorber in unit of  $10^{22} \text{ cm}^{-2}$ , <sup>d</sup> absorber ionization parameter ( $L/nR^2$ , see Done et al. 1992), <sup>e</sup> photon index <sup>f</sup>  $\chi^2$  for  $\Gamma$  fixed to 1.76, <sup>g</sup>, <sup>h</sup> and <sup>i</sup> as <sup>b</sup>, <sup>c</sup> and <sup>d</sup> respectively, for  $\Gamma$  fixed to 1.76.

complex absorption structure, namely the presence of an ionized absorber (models B and C).

Tables 4 and 5 report the best fit parameters of model B, obtained letting the continuum photon index free to vary and fixing it to its average value (the photon index is again consistent with a constant value during each observation).

The quality of the fits using model B, is significantly worse than that of model A. We used a simple equilibrium photoionization model ABSORI in XSPEC. Conversely, Schurch & Warwick (2002) argues that the variable absorber in NGC 4151 is often in a non-equilibrium ionization state. This may help in explaining the poor fits obtained with ABSORI. Interestingly, the ionization parameter of spectrum D of the 1996 July observation, when the source was in a high continuum state, is 2-10 times higher than that of spectra A and B, when the source was in a low state, although the errors are rather large. This behaviour is fully consistent with the warm absorber scenario.

Finally, we investigated model C, similar to that proposed by Piro et al. (2005). This produces ionization parameters consistent with zero in all cases, thus reproducing model A.

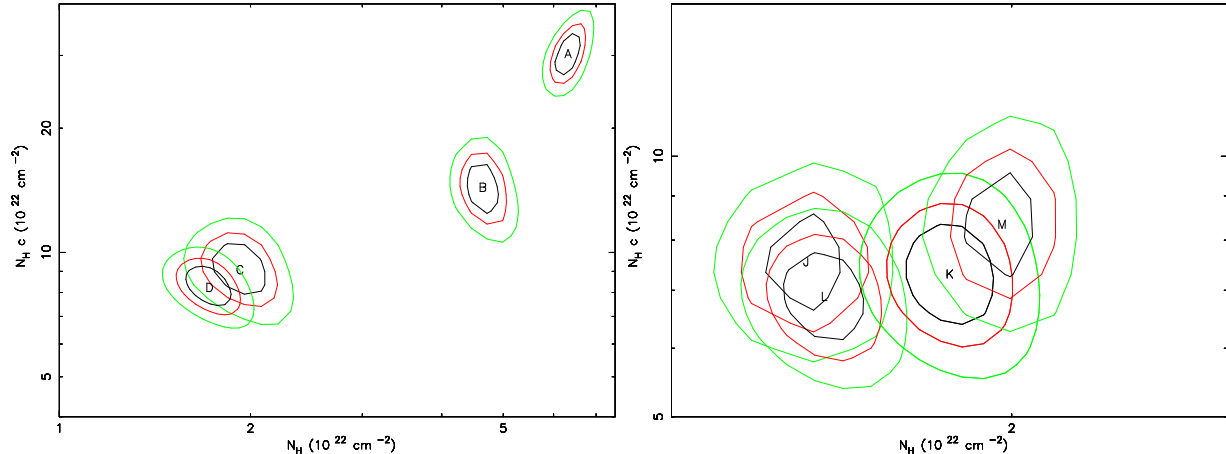


**Figure 8.** 68%, 90% and 99%  $\chi^2$  confidence contours of the partial covering absorber versus the totally covering absorber, from the fit with photon index and covering factor frozen. Left panel: 1996 July observation; right panel: 2001 December observation.

#### 4 DISCUSSION

We have analyzed two long (elapsed time  $\gtrsim 3$  days) BeppoSAX observations of NGC 4151 searching for variability of the absorber on time-scales from tens of ksec to years. We find significant low energy spectral variations in the softness ratio light curves of both observations suggesting that the absorption changed during the observations.

To characterize the spectral variability we used three models as a parameterization of the absorption: A) a partial covering absorber plus a uniform absorber, both neutral; B) one neutral absorber and one ionized absorber both covering the nucleus totally; and C) one ionized absorber covering the nucleus totally and one neutral absorber covering the nucleus only partly. The simplest partial covering model A provided the smallest  $\chi^2$  in both 1996 July and 2001 December observations. Factor of  $\sim 2$  changes of both the uniform and the partial covering absorbers have been obtained leaving the spectral index free to vary.

During the 2001 December observation the mean 6-10 keV count rate is only slightly higher than that of the low flux intervals of the 1996 July observations, but  $N_H$  and  $N_{HC}$  are a factor of about 3 smaller. They are also smaller than those in the 1996 July C and D intervals. Indeed the low energy absorption during the 2001 December observation is among the lowest ever measured in NGC 4151, as can be seen in figure 9, where we compare the best fit  $N_{HC}$  and  $c_v$  of the two BeppoSAX observations with a compilation of data from literature. The covering factor in the 2001 December observation appears lower than in all other historical observations with similar 2-10 keV flux. This suggests that on long time-scales (years) the variations of the covering factor are not (or not only) correlated with the X-ray continuum.

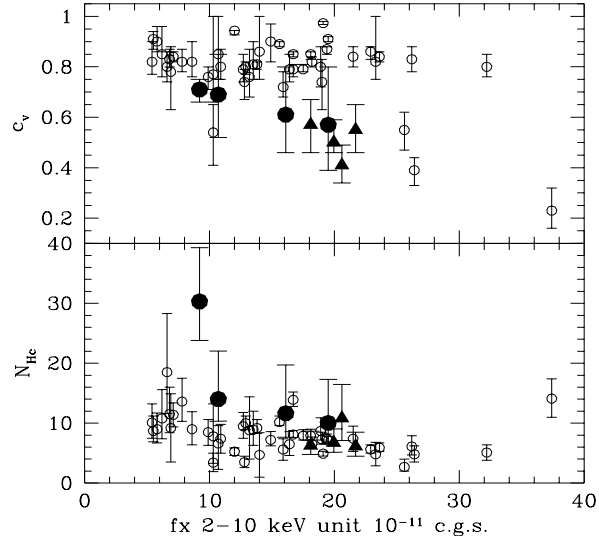


**Figure 9.** Upper panel: covering factor  $c_v$  versus the 2-10 keV flux. Bottom panel: column density  $N_{Hc}$  versus 2-10 keV flux. Solid dots identify the best fit values for the BeppoSAX 1996 July observation and the solid triangles identify the best fit values for the 2001 December observation. The open dots identify data from Pounds et al. 1986, Yaqoob, Warwick, & Pounds 1989, Fiore et al. 1990, Yaqoob & Warwick 1991, Yaqoob et al. 1993, Weaver et al. 1994, Warwick Done and Smith 1995, Zdziarski et al. 1996.

The partial covering model is a convenient parameterization, but does not have a direct physical interpretation. A more physical model is the clumpy absorber of Holt et al. (1980). In this model the absorbing medium is composed of a large number of small clouds, the column density of an individual cloud being  $n_c$  and the mean number of clouds along a particular line of sight being  $\mu$  (Holt et al. 1980). In this scenario, the observed variations of the column density are due to Poissonian fluctuations of the number of clouds,  $\mu$ . The covering factor  $c_v$  spans from  $\sim 0.4$  to  $\sim 0.9$  in  $\sim 50$  observations, with  $c_v \sim 0.2$  in only one case (figure 9). An immediate estimate of the probability of having no clouds along the line of sight is  $P(\mu = 0) = e^{-\mu} > 1/50$ , which implies  $\mu > 4$ . A better estimate can be obtained assuming a gaussian distribution of  $c_v$  around the average value  $\langle c_v \rangle \sim 0.65$ , with  $\sigma(c_v) \sim 0.15$ , implying  $\mu \sim 7$ .

During the 1996 July observation the largest variation of the column density is  $\sim 2 \times 10^{23} \text{ cm}^{-2}$  on time-scales as short as  $\sim 2$  days. This time-scale has strong implications for the location of the obscuring matter. Assuming that the absorbing medium is made by spherical clouds moving with Keplerian velocities around the central black hole ( $M_{BH} \sim 1.3 \times 10^7 M_\odot$ , Peterson et al. 2004), and identifying the above  $\sim 2$  days time-scale with the crossing time of a cloud, the absorbing medium would be located at the distance from the nucleus,  $r \leq 3.4 \times 10^4 (n_e)_{10}^2 t_2^2 R_S$ , where  $(n_e)_{10}$  is the density in units of  $10^{10} \text{ cm}^{-3}$ ,  $t_2$  is the time-scale

in units of two days and  $R_S$  is the Schwarzschild radius (Risaliti, Elvis & Nicastro 2002). If the X-ray absorber has a density typical of the clouds in the BELR,  $10^9 < n_e < 10^{11} \text{ cm}^{-3}$ , then it would be located at a distance from the nucleus  $340 R_S < r < 3.4 \times 10^6 R_S$ . This range includes the distance of the BELR, as inferred from reverberation mapping of the H $\beta$ , C IV, Mg II and H $\alpha$  line (Wandel, Peterson and Malkan 1999, Clavel et al. 1990, Sergeev 1994) and from theoretical estimates of the outer radius of the BELR (Cassidy and Raine 1997). If the X-ray absorber lies in the parsec scale dusty molecular torus (Krolik & Begelman 1988, Pier & Krolik 1992, Pier & Krolik 1993), its density would be  $n_e \gtrsim 5 \times 10^{10} \text{ cm}^{-3}$ . The X-ray absorber would then be a very compact slab (thickness  $\sim 1 R_S$ , i.e.  $\frac{\Delta R}{R} \sim 10^{-6}$ ) at parsec distance from the nucleus, which is a physically unlikely structure. We then conclude that the most likely location of the X-ray absorber is within the BELR. If the clouds absorbing the X-rays are pressure-confining by a hot medium surrounding the BELR, this confining gas would produce a thermal emission. Interpreting the 0.5-2 keV luminosity of the thermal bremsstrahlung during the December 2001 observation ( $\sim 10^{41} \text{ erg cm}^{-2} \text{ s}^{-1}$ ), as due to this confining gas, the size of the region containing the thermal gas is  $1 \times 10^4 T_7^{-1/3} n_7^{-2/3} R_S$ , where  $T_7$  and  $n_7$  are the temperature and the density in units of  $10^7 \text{ K}$  and  $10^7 \text{ cm}^{-3}$  respectively. This is consistent with the distance from the nucleus of the BELR, and therefore a pressure-confining medium can not be excluded.

Variations of the X-ray absorber on time-scales of days are expected in the model proposed by Elvis (2000) for type 1 AGN and extended to type 2 AGN by Risaliti, Elvis & Nicastro (2002). In the model of Elvis (2000), a wind arises vertically from a narrow region on the accretion disk and it is then radially accelerated by the radiation pressure (Murray et al. 1995, Kartje, Königl & Elitzur 1999). The wind is both warm ( $\sim 10^6 \text{ K}$ ) and highly ionized, with a density  $n_e \sim 10^7 \text{ cm}^{-3}$ , which puts it in pressure equilibrium with the BELR clouds. The BELR is then a cool phase embedded in the wind and absorbing the X-rays coming from the nucleus. In the wind model the X-rays absorber is axisymmetric, like the torus, but the typical size and dynamic state in the two cases are quite different. In particular the X-ray absorber is located a few light days from the nucleus, then changes of the column density and/or of the covering factor are naturally expected on time-scales greater than a few days. Elvis et al. (2004) have found a factor of 100 decrease in the column density toward the normally almost Compton-thick ( $\tau \sim 0.1\text{-}0.3$ ) type 2 AGN NGC 4388 on time-scales either  $\sim 2$  days or 4 hr, thus giving further support to the “wind” model. Such model naturally predicts an absorber made by a cold and a warm phase.

We tested this scenario through our models B and C. The best fit ionization parameters are roughly in the range found by Schurch & Warwick (2002). Although the behaviour of the ionization parameter in model B is nicely consistent with the expectations, with the absorber ionization parameter  $\xi$  roughly correlated with the intrinsic flux, the results are not satisfactory from the statistical point of view, indicating that the physical and geometrical structure of the absorber is more complex than any of our simple parameterizations. Model C, similar to that proposed by Piro et al. (2005) produces best fit ionization parameters consistent with zero in all cases, thus reproducing model A. In particular, our time dependent spectral analysis does not confirm the Piro et al. (2005) claim of a significant highly ionized iron absorption feature. Therefore a word of caution should be spent about the presence of a relativistic outflow in this source.

To better locate the X-rays absorber, long monitoring of the source with instruments with good energy resolution and high sensitivity (to collect high quality spectra in a few thousands of seconds) are needed. Simultaneous optical monitoring of the source would allow us to search for dust features, and therefore to understand how much dust lies in the region occupied by the X-ray absorber. Simultaneous X-ray and optical-UV spectroscopy could also be used to investigate whether broad emission lines emerge when the column density of the absorber along the line of sight is decreasing. X-ray spectroscopy on short time-scales ( $\sim 1$  ksec) could also be used to determine whether the change of the absorbing column is step-wise (as expected for discrete clouds with sharp edges) or more continuous, by giving a measure of the 'fuzziness' of the clouds (i.e. their column density gradients).

### Acknowledgements

This work was partially supported from NASA grant G02-3142X. We thank Giuseppe Cesare Perola for useful discussions.

## REFERENCES

- Antonucci, R. 1993 *ARA&A*, 31, 47
- Barr, P.; White, N. E.; Sanford, P. W 1977, *MNRAS*, 181, 43
- Barvainis R. 1987, *ApJ*, 320, 537
- Boella, G.; Chiappetti, L.; Conti, G. et al. 1997, *A&AS*, 122, 299
- Burstein, D.; Jones, C.; Forman, W. et al. 1997, *ApJS*, 111, 163
- Done, C.; Mulchaey, J. S.; Mushotzky, R. F. et al. 1992, *ApJ*, 395, 275

Canizares, C. R.,<http://space.mit.edu/HETG/>

Cassidy I. and Raine D. J. 1997, *A& A* 322, 400

Clavel, J.; Boksenberg, A.; Bromage, G. E. et al. 1990, *MNRAS*, 246, 668

Elvis, M., Schreier, E. J., Tonry, J. et al. 1981 *ApJ*, 246, 20

Elvis, M.; Briel, U. G.; Henry, J. P. 1983, *ApJ*, 268, 105

Elvis, M.; Fassnacht, C.; Wilson, A. S.; Briel 1990, *ApJ*, 361, 459

Elvis, M. 2000 *ApJ* 545, 63

Elvis M., Risaliti G., Nicastro N. et al. 2004, *ApJ*, 615L, 25

Fabbiano, G.; Kim, D.-W.; Trinchieri, G. 1992, *ApJS*, 80, 531

Fiore, F.; Perola, G. C.; Romano, M. 1990, *MNRAS*, 243, 522

Fiore, F., Guainazzi, M. & Grandi, P. 1999, Handbook for BeppoSAX NFI spectral analysis,[ftp://ftp.asdc.asi.it/pub/sax/doc/software\\_docs/saxabc\\_v1.2.ps.gz](ftp://ftp.asdc.asi.it/pub/sax/doc/software_docs/saxabc_v1.2.ps.gz) or [http://heasarc.gsfc.nasa.gov/docs/sax/abc/saxabc/saxabc\\_v1.2.ps.gz](http://heasarc.gsfc.nasa.gov/docs/sax/abc/saxabc/saxabc_v1.2.ps.gz)

Frontera, F.; Costa, E.; dal Fiume, D. et al. 1997, *A&AS*, 122, 357

Gioia, I. M.; Maccacaro, T.; Schild, R. E. et al. 1990, *ApJS*, 72, 567

Gursky, H.; Kellogg, E. M.; Leong, C. et al. 1971, *ApJ*, 165L, 43

Holt, S. S.; Mushotzky, R. F.; Boldt, E. A. et al. 1980, *ApJ*, 241L, 13

Ives, J. C. Sandford, P. W. & Penston, M. V., 1976, *AJ*, 207, 159

Johnson, W. N.; McNaron-Brown, K.; Kurfess, J. D. et al. 1997, *ApJ*, 482, 173

Kartje, J. F., Königl, A. & Elitzur, M. 1999, *ApJ*, 513, 180

Krolik, J. H. & Begelman M. C. 1988, *ApJ*, 329, 702

Lampton M., Margon B. & Bowyer S., 1976, *ApJ* 208, 1771

Lawrence, A. & Elvis, M. 1982, *ApJ*, 256, 410

Magdziarz, P. & Zdziarski, A. A. 1995, *MNRAS*, 273, 837

Murray, N., Chiang, J., Grossman, S. A. et al. 1995 *ApJ*, 451, 498

Nicastro, F.; Fiore, F.; Perola, G. C.; Elvis, M. 1999, *ApJ*, 512, 184

Ogle, P. M.; Marshall, H. L.; Lee, J. C. et al. 2000, *ApJ*, 545, 81

Paciesas, W. S.; Mushotzky, R. F. & Pelling, R. M. 1997, *MNRAS*, 178, 23

Parmar, A. N.; Martin, D. D. E.; Baudaz, M. et al. 1997, *A&AS*, 122, 309

Pearson, J. F., Bannister, N. P.; Fraser, G. W.; The Lobster-ISS Consortium 2003, *AN*, 324, 168

Perlman E. S., Stocke, J. T., Wang, Q. D. et al. 1996, *ApJ*, 456, 451

Perola, G. C.; Piro, L.; Altamore, A. et al. 1986, *ApJ*, 306, 508

Peterson, B. M.; Ferrarese, L.; Gilbert, K. M. et al. 2004, ApJ, 613, 682

Pounds, K. A.; Warwick, R. S.; Culhane, J. L. et al. 1986, MNRAS, 218, 685

Pier, E. A. & Krolik, J. H. 1992 ApJ, 399L, 23

Pier, E. A. & Krolik, J. H. 1993 ApJ, 418m 673

Risaliti, G.; Elvis, M.; Nicastro, F. 2002 ApJ, 571, 234

Takahashi, K.; Inoue, H. and Dotani T., 2002, PASJ, 54, 373

Schurch, N. J. and Warwick, R. S. 2002, MNRAS, 334, 811

Schurch, N. J.; Warwick, R. S.; Griffiths R. E. et al 2003, MNRAS, 345, 423

Sergeev, S. G. 1994, ARep, 38, 162

Smith, D. A.; Georgantopoulos, I.; Warwick, R. S. 2001, ApJ, 550, 635

Urry & Padovani 1995, PASP, 107, 803

Yaqoob, T.; Warwick, R. S.; Pounds, K. A 1989, MNRAS, 236, 153

Yaqoob, T. and Warwick, R. S. 1991, MNRAS, 248, 773

Yaqoob, T.; Warwick, R. S.; Makino, F. et al. 1993, MNRAS, 264, 411

Yang, Y.; Wilson, A. S.; Ferruit, P. et al. 2001, ApJ, 563, 124

Wandel, A.; Peterson, B. M. and Malkan, M. A. 1999, ApJ, 526, 579

Warwick R. S., Done C. and Smith D. A. 1995 MNRAS, 275, 1003

Weaver, K. A.; Yaqoob, T.; Holt, S. S. et al. 1994, ApJ, 436L, 27

Zdziarski, A. A.; Johnson, W. N.; Magdziarz, P. 1996, MNRAS, 283, 193

Zdziarski, A. A.; Leighly, K. M.; Matsuoka, M. et al. 2002, ApJ, 573, 505